

Emergence of dynamical complexity related to human heart rate variabilityMei-Chu Chang,^{1,2} C.-K. Peng,³ and H. Eugene Stanley²¹*Center for Dynamical Biomarkers and Translational Medicine, National Central University, Zhongli 32001, Taiwan*²*Center for Polymer Studies and Department of Physics, Boston University, Boston, Massachusetts 02215, USA*³*Cardiovascular Division and Margret and H. A. Rey Institute for Nonlinear Dynamics in Medicine, Beth Israel Deaconess Medical Center/Harvard Medical School, Boston, Massachusetts 02215, USA*

(Received 4 October 2014; published 9 December 2014)

We apply the refined composite multiscale entropy (MSE) method to a one-dimensional directed small-world network composed of nodes whose states are binary and whose dynamics obey the majority rule. We find that the resulting fluctuating signal becomes dynamically complex. This dynamical complexity is caused (i) by the presence of both short-range connections and long-range shortcuts and (ii) by how well the system can adapt to the noisy environment. By tuning the adaptability of the environment and the long-range shortcuts we can increase or decrease the dynamical complexity, thereby modeling trends found in the MSE of a healthy human heart rate in different physiological states. When the shortcut and adaptability values increase, the complexity in the system dynamics becomes uncorrelated.

DOI: [10.1103/PhysRevE.90.062806](https://doi.org/10.1103/PhysRevE.90.062806)

PACS number(s): 89.75.Hc, 05.40.Ca, 05.45.Tp

I. INTRODUCTION

Physiological systems regulated by underlying mechanisms associated with multiple spatiotemporal scales exhibit extraordinary complexity with nonstationary and nonlinear behavior [1–4]. A powerful entropy-based method—multiscale entropy (MSE)—was developed to define the *dynamical complexity* of a complex system, i.e., to express how well a complex system can adapt itself to a challenging environment [5–7]. The algorithm has been widely applied to living systems experiencing a variety of physiological states and pathologic conditions over a range of temporal scales [5–15]. For example, when we apply MSE to human heart rate variability (HRV) we find that the HRV of healthy young adults exhibits the highest complexity and that aging and disease reduce that complexity [5–7]. The normal fetal HRV for a mature gestational age exhibits a higher complexity than that for earlier gestational ages [8]. However the mechanisms that underlie (i) the high complexity for the healthy physiological young state and (ii) the low complexity for the aging and developmental states remain unknown.

Complex systems can be described topologically as complex networks with nodes representing individual components and links representing the interactions among them [16–19]. Small-world (SW) networks [19,20] have motivated studies in different fields, such as human brains [21–26]. Exploring collective dynamical behavior of the SW network through the interplay between the intrinsic dynamics of the constituent nodes and the topology is also important [27–42]. It is still an open issue of how the dynamical complexity of a SW system with fluctuating signals can be achieved and can be physiologically related, especially when each node represents a multicomponent complex system with its own regulatory mechanism.

In this work, we report that in a one-dimensional directed SW network composed of nodes whose states are binary and whose dynamics obey the majority rule (see below), the dynamical complexity of the SW network emerges by applying a refined composite MSE algorithm [43]. Unlike the conventional studies concerning the mean field of SW systems,

fluctuations from the mean field are emphasized here. We find that the coexistence of short-range connections and long-range shortcuts and the presence of the system “adaptability” from the noisy environment make the SW system reach high dynamical complexity. Lower or higher adaptability decreases the complexity of system. Increasing long-range shortcuts can lead to the increase of system complexity. The change of complexity by tuning the adaptability and long-range shortcuts exhibits a trend similar to that found in the healthy human HRV under different states, e.g., young, aging, and developmental states. Further, both large values of adaptability and a great amount of shortcuts make the fluctuation of the SW system become uncorrelated. Such a simple model is suitable to capture essential features of the more complicated processes taking place in real physiological systems.

II. THE MODEL

To construct a directed SW network, we start with an N -node one-dimensional ring, in which each node is connected with its two nearest neighbors by two incoming and two outgoing links. Instead of rewiring links with probability p [19], we add excess long-range directed links (shortcuts) $f_e N$ in the ring structure by randomly choosing two nonconnected nodes (thus f_e is the mean excess degree). The average incoming and outgoing degrees are equal to $2 + f_e$. Note that the reason for adding directed links to the system is due to the asymmetry in a real system. In this way, a network with long-range directed shortcuts is obtained [for example, the system size $N = 100$ and the mean excess degree $f_e = 0.2$ in Fig. 1(a)].

Second, the states of nodes in this SW network can simply be one of two possible states, just as the excitatory and inhibitory of neurons in brain, the increase and decrease of respiratory rate, the elevation and drop of blood pressure, and so on. Therefore, the state of every node i can be described by a spinlike variable $\sigma_i = +1$ or -1 . Then, the interactions between nodes obey the majority rule. For each iteration, the temporal state σ_i of node i at time $t + 1$ can be determined according to the majority rule at time t , i.e., $\sigma_i(t + 1) =$

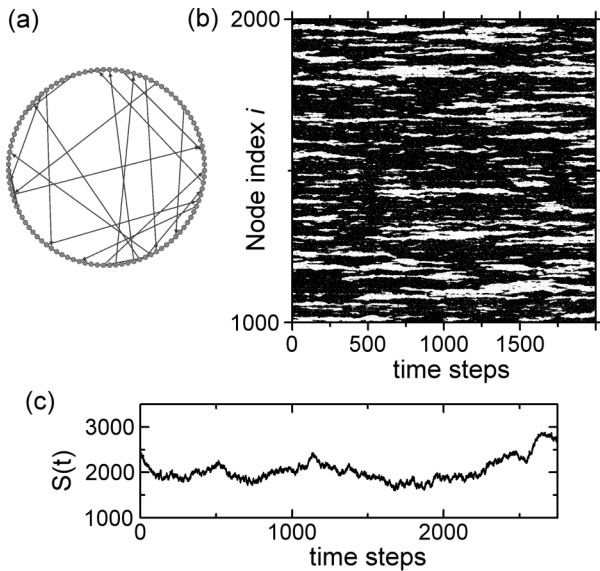


FIG. 1. (a) An illustration of the structure of a one-dimensional directed SW network, where the system size $N = 100$ and the mean excess degree $f_e = 0.2$. (b) The temporal state fluctuation of nodes $i = 1000, \dots, 2000$ after waiting a transient 8192 time steps, where $N = 4096$, $f_e = 0.2$, and $\Pi_n = 0.2$. White and black regions represent $\sigma_i(t) = -1$ and $+1$, respectively. (c) The system dynamical behavior $S(t) = \sum_{i=1}^{4096} \sigma_i(t)$, where $f_e = 0.2$ and $\Pi_n = 0.2$.

$\text{sgn}[\sum_{j \in \{i\}} \sigma_j(t)]$, where the sum runs over the connected nodes σ_j at time t . If the sum equals zero, node i keeps its own state; i.e., $\sigma_i(t+1) = \sigma_i(t)$.

Third, the adaptability (Π_n) of the SW system to the noisy environment is introduced and also can be interpreted as the noise strength. Each link from node j to i has a probability Π_n to be assigned one of two possible states ± 1 , chosen at random with probability $1/2$, instead of transmitting the true signal. In other words, at each time step, there are $\Pi_n \times (2N + f_e N)$ links randomly chosen to fail to communicate signals between nodes, but these links can still receive the stimulus from the environment. Why is the adaptability Π_n defined in such a way? In the noisy environment, a healthy system should be able to adapt itself by carrying “noisy” information within the interactions between nodes. The system allows the communication between nodes affected by external noisy stimulus [44]. This explains why a healthy system with a proper adaptability Π_n exhibits high complexity in a challenging environment [5–7].

III. METHODS

We choose system size $N = 4096$. Initially, the state $\sigma_i(t=0)$ of each node $i = 1, \dots, 4096$ is randomly chosen to be $+1$ or -1 . Waiting for a transient period lasting 8192 time steps, we then record the temporal node states for an additional 60 000 time steps. Figure 1(b) shows the temporal state fluctuation of some nodes $i = 1000, \dots, 2000$, where $f_e = 0.2$ and $\Pi_n = 0.2$. Here, the dynamical behavior is defined as $S(t) = \sum_{i=1}^{4096} \sigma_i(t)$. Figure 1(c) is the system dynamical behavior $S(t)$ when $f_e = 0.2$ and $\Pi_n = 0.2$.

We are interested in the fluctuation of $S(t)$ which is processed by the empirical mode decomposition (EMD) method, a nonlinear, nonstationary signal processing tool [45]. The basic idea of EMD is to decompose the original time signal into components, namely, intrinsic mode functions (IMFs), which are suitable for defining a meaningful instantaneous frequency. These IMFs have the same numbers of extrema and zero crossings, and they are symmetric with respect to local zero mean. The extraction of IMFs is achieved by means of a decomposition based on the assumptions that the signal has at least one maximum and one minimum. After applying the EMD method, the signal $S(t)$ can be expressed as $S(t) = \sum_{i=1}^n \text{IMF}_i + r_n$, where the final residue r_n can be interpreted as either the mean trend of $S(t)$ or a constant value. Thus, the fluctuating signal $S'(t) = \sum_{i=1}^n \text{IMF}_i = S(t) - r_n$ is calculated and then used to identify the dynamical complexity of the SW system by a refined composite MSE method [43].

The MSE method [5–7] quantifies the dynamical complexity from fluctuating time series by the following steps. (i) Coarse-grained time series are constructed by dividing the original time series into nonoverlapping windows of length τ and averaging data points inside each window. (ii) For each coarse-grained time series, the sample entropy (SampEn) quantifying the regularity is calculated. It reflects the conditional probability that two sequences of m consecutive data points which are similar to each other will remain similar when the next point is included. The sample entropy of a given sequence $x(t)$ is defined as the natural logarithm of the ratio of n^m to n^{m+1} , i.e., $\text{SampEn}[x(t), m, r] = -\ln(n^{m+1}/n^m)$, where r is the a predefined tolerance, and n^{m+1} and n^m are the total number of $(m+1)$ - and m -component matches, respectively. Then, the SampEn is plotted as a function of the time scale factor τ .

Recently, a refined composite MSE (RCMSE) was developed in order to improve the accuracy of the MSE due to the coarse-graining procedure reducing the length of a time series considerably at large scales [43]. In this paper, all sample entropies are given by the RCMSE algorithm with the same conditions in [6] ($m = 2$, $r = 0.15$).

IV. RESULTS

How does the complexity of a healthy subject look physiologically? The clinical cardiac interbeat (RR) interval time series of healthy subjects were gathered from 24-hour Holter monitor recordings of 72 healthy subjects with ECG data sampled at 128 Hz (from the PhysioNet database [46,47]). We choose two control groups from the database: (i) 14 young subjects, 7 men and 7 women, aged 30.5 ± 4.4 years (mean \pm SD), range 20–35 years, and (ii) 16 elderly subjects, 9 men and 7 women, aged 70.0 ± 3.1 years (mean \pm SD), range 68–76 years. Within the 24-hour data, only the data for the groups during waking period are focused by extracting the segments of 3×10^4 consecutive data points with highest heart rate. Similarly, we apply each RR series to the EMD method ($n = 13$), and obtain the revised RR series ($\text{RR}' = \sum_{i=1}^8 \text{IMF}_i$) by removing the trend (in this case, the last five modes and r_n) [11].

Figure 2(a) shows the sample entropy of the revised RR series (RR') of healthy young subjects using the RCMSE

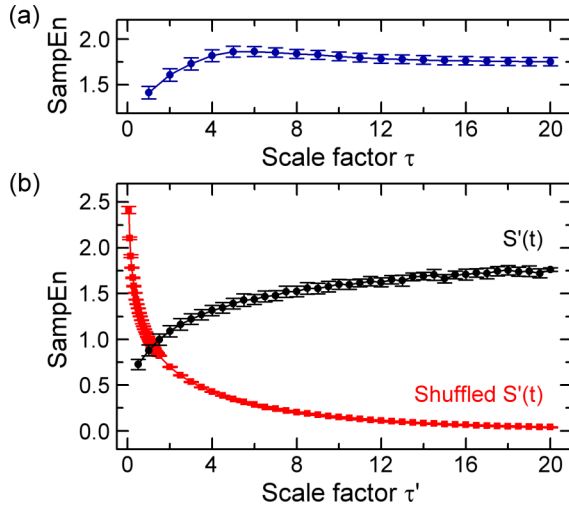


FIG. 2. (Color online) (a) The sample entropy (SampEn) of revised RR' time series of 14 healthy young people during waking period, 7 men and 7 women, aged 30.5 ± 4.4 years (mean \pm SD), range 20–35 years. Symbols represent the average values of sample entropy, and the bars are the standard error. The time series length is 3×10^4 beats. (b) The black circles showing the sample entropy of fluctuating $S'(t)$ by RCMSE from scale factor $\tau = 10$ –400, where $f_e = 0.2$, $\Pi_n = 0.1$, and the rescaled τ' is given by dividing τ by 20. The red squares depict the entropy results from the shuffled $S'(t)$. Each symbol is averaged by ten rounds. The bars are the standard error.

method for different time scale factors $\tau = 1$ –20. For large scales [e.g., $\tau \geq 5$; Fig. 2(a)], the RR' series of healthy young subjects are assigned the highest entropy values. The sample entropy value reaches about 1.75 at large τ . Figure 3(a) is the comparison of sample entropy of RR' series between young and elderly groups. It shows that an aging healthy subject leads to loss of complexity, i.e., the lower entropy values over all scale factors.

Does our SW model exhibit such a phenomenon in which its complexity remains high or decreases under different parameters? In Fig. 2(b), black circles show the sample entropy of $S'(t)$ from the RCMSE method for $\tau = 10$ –400, where $f_e = 0.2$, $\Pi_n = 0.1$, and the rescaled τ' is given by dividing τ by 20. Each circle is the mean value obtained by averaging ten rounds under the same condition. The error bars are the standard error. The red squares in Fig. 2(b) depict that the entropy drops to zero are large scales once the $S'(t)$ is shuffled. Note that in the simulation, we do not introduce any specific time scales. By rescaling the scale factors from τ to τ' , the entropy value of $S'(t)$ in Fig. 2(b) at large scales is similar to that of RR' of healthy subjects shown in Fig. 2(a). It is interesting to see, once the scales are fixed, how the complexity of the SW system evolves when f_e and Π_n change.

In Fig. 3(a), a healthy system with aging leads to the loss of complexity over different time scales. The system loses its adaptability for a challenging environment. In our model [Fig. 3(b)], the entropy of $S'(t)$ decreases when $\Pi_n < 0.1$. It means that when the SW system loses its adaptability to a noisy environment, its dynamical complexity can decrease also. Will the complexity increase if the system allows $\Pi_n >$

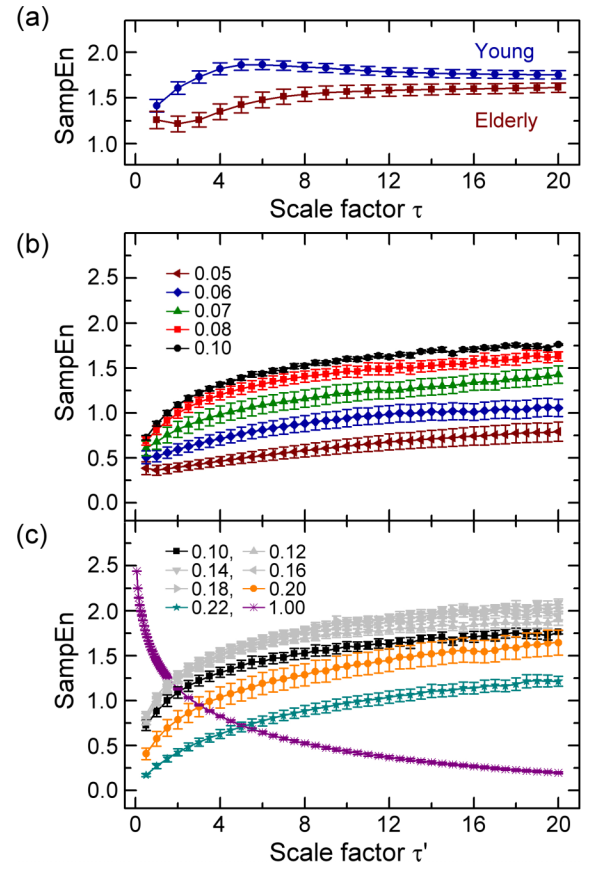


FIG. 3. (Color online) (a) The sample entropy (SampEn) of revised RR' series of 14 healthy young subjects (blue circles) and the 16 healthy elderly subjects (wine squares) during waking period. The 16 healthy elderly subjects are 9 men and 7 women, aged 70.0 ± 3.1 years (mean \pm SD), range 68–76 years (t -test, $p < 0.05$). Symbols represent the average values of sample entropy, and the bars are the standard error. The time series length is 3×10^4 beats. The entropy of elderly subjects is lower than that of young subjects over all scale factors. (b) and (c) The sample entropy of $S'(t)$ for $\Pi_n = 0.05$ –0.10, $\Pi_n = 0.10$ –0.22, and $\Pi_n = 1.0$, where $f_e = 0.2$, $\tau = 10$ –400, and the rescaled τ' is given by dividing τ by 20. Each symbol is averaged by ten rounds. The bars are the standard error.

0.1? Figure 3(c) shows that the entropy will increase first to about 2.0 at $\tau' = 20$ when $\Pi_n > 0.1$, but then it will decrease when Π_n is larger. Eventually, $S'(t)$ is uncorrelated at $\Pi_n = 1.0$, and the entropy drops close to zero at large τ' .

Figure 4 shows the complexity index by summing sample entropy in Figs. 3(b) and 3(c), where black squares and blue circles represent the sum of the entropy from $\tau' = 1$ –10 and $\tau' = 11$ –20, respectively. We find that the SW system can exhibit high complexity with large entropy under a proper range of Π_n . Above or beyond the proper range of Π_n , the complexity of the SW system will decrease.

Another interesting question is how a healthy subject increases its complexity when it is in its developmental state. Physiologically, for example, the normal fetal HRV at mature gestational age exhibits higher complexity than that at earlier gestational age [8]. Intuitively, this means that the coupling strength increases when the system grows. Thus, in our model, the increasing coupling strength is represented as the increase

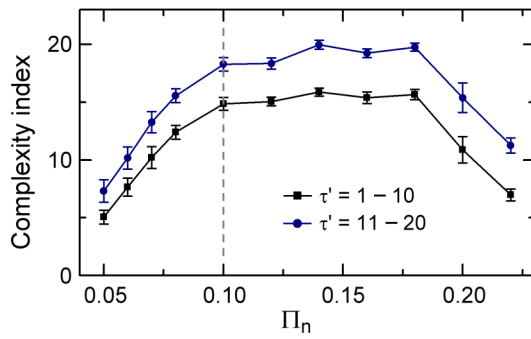


FIG. 4. (Color online) The complexity index obtained by summing the area of sample entropy in Figs. 3(b) and 3(c). Squares and circles represent the range for $\tau' = 1-10$ and $11-20$, respectively. The bars are the standard error.

of long-range shortcuts when the complex system develops. Figure 5(a) depicts how we develop an $N = 100$ SW system by adding f_e . The SW network at $f_e = 0.12$ in the middle panel of Fig. 5(a) is constructed by adding $\Delta f_e N$ to the SW network at $f_e = 0.08$ in the left panel, where $\Delta f_e = 0.04$. Adding next $\Delta f_e N$ shortcuts to the SW network at $f_e = 0.12$ leads to the SW network in the right panel of Fig. 5(a). Figure 5(b) is the corresponding sample entropy for $f_e = 0.08, 0.12, 0.16, 0.20$, and 1.00 . It is found that the complexity increases when f_e increases at fixed Π_n . Note that when $f_e = 1$, the complexity drops fast and is less correlated. The effect of larger f_e is similar to the effect of large Π_n .

V. DISCUSSION

Through the interplay between the intrinsic dynamics of the nodes and SW topology, the dynamical behavior of SW system can be observed. The ferromagnetic transition in SW networks with the Ising model [28–30], the epidemic spread and opinion formation in SW social networks [31–36], the self-sustained synchronization in SW neuron networks [37–40], and $1/f$ fluctuating signals in SW Boolean networks [41,42] are good examples.

In this work, the dynamical complexity of a SW system with fluctuating signals is achieved and can be physiologically related to human heart rate variability. We constructed a one-dimensional directed SW network composed of binary nodes whose interactions obey the majority rule. The dynamical

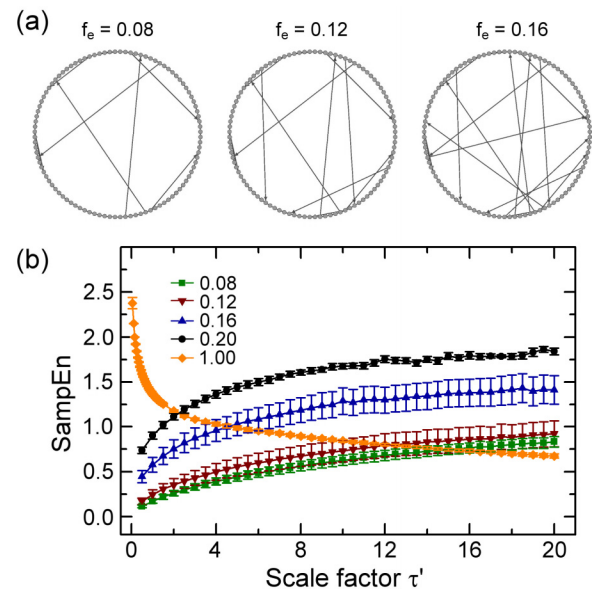


FIG. 5. (Color online) (a) The panels of how to develop a SW network by adding $\Delta f_e N$ long-range links to make $f_e = 0.08$ (left), 0.12 (middle), and 0.16 (right), where $N = 100$ and $\Delta f_e = 0.04$. (b) The corresponding sample entropy (SampEn) of $S'(t)$ for $f_e = 0.08, 0.12, 0.16, 0.20$, and 1.00 , where $\Pi_n = 0.10$, $\tau = 10-400$, and the rescaled τ' is given by dividing τ by 20. Each symbol is averaged by ten rounds. The bars are the standard error.

complexity can be observed by focusing on the fluctuation and applying the RCMSE analysis. (i) The existence of long-range links and the proper adaptability Π_n of a noisy environment lead to high complexity. (ii) The increase and decrease of Π_n result in the drop of complexity. Only a proper regime of adaptability allows the SW system with high complexity. For $\Pi_n = 1$, the fluctuating signal becomes uncorrelated. (iii) The increase of f_e also leads to the increase of complexity, similar to a developing healthy system. A larger f_e also leads to the loss of complexity. The effect of larger f_e is similar to the effect of larger Π_n .

ACKNOWLEDGMENTS

This work is supported by the NSC support for the Center for Dynamical Biomarkers and Translational Medicine, National Central University, Taiwan (NSC 102-2911-I-008-001) and by the Postdoctoral Research Abroad Program, National Science Council, Taiwan (NSC 102-2917-I-564-056).

[1] J. B. Bassingthwaite, L. S. Liebovitch, and B. J. West, *Fractal Physiology* (Oxford University Press, New York, 1994).
 [2] G. B. West, J. H. Brown, and B. J. Enquist, *Science* **276**, 122 (1997).
 [3] A. L. Goldberger, L. A. N. Amaral, J. M. Hausdorff, P. C. Ivanov, C.-K. Peng, and H. E. Stanley, *Proc. Natl. Acad. Sci. USA* **99**, 2466 (2002).

[4] C.-K. Peng, J. Mietus, J. M. Hausdorff, S. Havlin, H. E. Stanley, and A. L. Goldberger, *Phys. Rev. Lett.* **70**, 1343 (1993).
 [5] M. Costa, A. L. Goldberger, and C.-K. Peng, *Phys. Rev. Lett.* **89**, 068102 (2002).
 [6] M. Costa, A. L. Goldberger, and C.-K. Peng, *Phys. Rev. E* **71**, 021906 (2005).

- [7] C.-K. Peng, M. Costa, and A. L. Goldberger, *Adv. Adapt. Data Anal.* **01**, 61 (2009).
- [8] D. Hoyer, S. Nowack, S. Bauer, F. Tetschke, S. Ludwig, L. Moraru, A. Rudolph, U. Wallwitz, F. Jaenicke, J. Haueisen, E. Schleubner, and U. Schneider, *Comput Biol. Med.* **42**, 335 (2012).
- [9] M. Ferrario, M. G. Signorini, and G. Magenes, *Med. Biol. Eng. Comput.* **47**, 911 (2009).
- [10] M. Costa, C.-K. Peng, A. L. Goldberger, and J. M. Hausdorff, *Physica A* **330**, 53 (2003).
- [11] B. Manor, M. Costa, K. Hu, E. Newton, O. Starobinets, H. G. Kang, C.-K. Peng, V. Novak, and L. A. Lipsitz, *J. Appl. Physiol.* **109**, 1786 (2010).
- [12] J. Escudero, D. Abásolo, R. Hornero, P. Espino, and M. López, *Physiol. Meas.* **27**, 1091 (2006).
- [13] T. Takahashi, R. Y. Cho, T. Mizuno, M. Kikuchi, T. Murata, K. Takahashi, and Y. Wada, *NeuroImage* **51**, 173 (2010).
- [14] A. R. McIntosh, N. Kovacevic, and R. J. Itier, *PLoS Comput. Biol.* **4**, e1000106 (2008).
- [15] P.-F. Lin, M. T. Lo, J. Tsao, Y.-C. Chang, C. Lin, and Y.-L. Ho, *PLoS ONE* **9**, e87798 (2014).
- [16] R. Albert and A.-L. Barabási, *Rev. Mod. Phys.* **74**, 47 (2002).
- [17] S. N. Dorogovtsev and J. F. F. Mendes, *Adv. Phys.* **51**, 1079 (2002).
- [18] M. E. J. Newman, *SIAM Rev.* **45**, 167 (2003).
- [19] D. J. Watts and S. H. Strogatz, *Nature (London)* **393**, 440 (1998).
- [20] A small-world network interpolates between regular lattices and fully random graphs by randomly creating some long-range shortcuts.
- [21] E. Bullmore and O. Sporns, *Nat. Rev. Neurosci.* **13**, 336 (2012).
- [22] E. Bullmore and O. Sporns, *Nat. Rev. Neurosci.* **10**, 186 (2009).
- [23] D. S. Bassett and E. Bullmore, *Neuroscientist* **12**, 512 (2006).
- [24] T. Uehara, T. Yamasaki, T. Okamoto, T. Koike, S. Kan, S. Miyauchi, J. Kira, and S. Tobimatsu, *Cereb. Cortex* **24**, 1529 (2014).
- [25] E. J. Sanz-Arigita, M. M. Schoonheim, J. S. Damoiseaux, S. A. R. B. Rombouts, E. Maris, F. Barkhof, P. Scheltens, and C. J. Stam, *PLoS ONE* **5**, e13788 (2010).
- [26] W. Liao, Z. Zhang, Z. Pan, D. Mantini, J. Ding, X. Duan, C. Luo, G. Lu, and H. Chen, *PLoS ONE* **5**, e8525 (2010).
- [27] S. H. Strogatz, *Nature (London)* **410**, 268 (2001).
- [28] C. P. Herrero, *Phys. Rev. E* **65**, 066110 (2002).
- [29] A. D. Sánchez, J. M. López, and M. A. Rodríguez, *Phys. Rev. Lett.* **88**, 048701 (2002).
- [30] A. Barrat and M. Weigt, *Eur. Phys. J. B* **13**, 547 (2000).
- [31] C. Moore and M. E. J. Newman, *Phys. Rev. E* **61**, 5678 (2000).
- [32] M. Kuperman and G. Abramson, *Phys. Rev. Lett.* **86**, 2909 (2001).
- [33] P.-P. Li, D.-F. Zheng, and P. M. Hui, *Phys. Rev. E* **73**, 056128 (2006).
- [34] L.-L. Jiang, D.-Y. Hua, J.-F. Zhu, B.-H. Wang, and T. Zhou, *Eur. Phys. J. B* **65**, 251 (2008).
- [35] D. H. Zanette, *Phys. Rev. E* **65**, 041908 (2002).
- [36] C. Castellano, S. Fortunato, and V. Loreto, *Rev. Mod. Phys.* **81**, 591 (2009).
- [37] L. F. Lago-Fernández, R. Huerta, F. Corbacho, and J. A. Sigüenza, *Phys. Rev. Lett.* **84**, 2758 (2000).
- [38] A. Roxin, H. Riecke, and S. A. Solla, *Phys. Rev. Lett.* **92**, 198101 (2004).
- [39] Q. Wang, M. Perc, Z. Duan, and G. Chen, *Physica A* **389**, 3299 (2010).
- [40] H. Yu, J. Wang, C. Liu, B. Deng, and X. Wei, *Physica A* **392**, 5473 (2013).
- [41] L. A. N. Amaral, A. Diaz-Guilera, A. A. Moreira, A. L. Goldberger, and L. A. Lipsitz, *Proc. Natl. Acad. Sci. U.S.A.* **101**, 15551 (2004).
- [42] A. Díaz-Guilera, A. A. Moreira, L. Guzman, and L. A. N. Amaral, *J. Stat. Mech. Theor. Exp.* (2007) P01013.
- [43] S.-D. Wu, C.-W. Wu, S.-G. Lin, K.-Y. Lee, and C.-K. Peng, *Phys. Lett. A* **378**, 1369 (2014).
- [44] D. J. Mar, C. C. Chow, W. Gerstner, R. W. Adams, and J. J. Collins, *Proc. Natl. Acad. Sci. USA* **96**, 10450 (1999).
- [45] N. E. Huang, Z. Shen, S. R. Long, M. C. Wu, H. H. Shih, Q. Zheng, N.-C. Yen, C. C. Tung, and H. H. Liu, *Proc. R. Soc. A* **454**, 903 (1998).
- [46] See <http://www.physionet.org/physiobank/database/nsrdb>.
- [47] See <http://www.physionet.org/physiobank/database/nsr2db>.